

Magnetostatic response and field-controlled haloing in binary superparamagnetic mixtures

Andrey A. Kuznetsov*

The work is devoted to the theoretical and numerical analysis of a two-component superparamagnetic system. Namely, of a rigid superparamagnetic cluster embedded in a superparamagnetic medium and subjected to a uniform magnetic field. Both cluster and the medium contain single-domain nanoparticles of the same diameter and magnetic moment. But the concentration of nanoparticles within the cluster is higher than that in the surrounding medium. Equilibrium magnetic response of the system in wide ranges of concentrations and interaction energies is calculated using Langevin dynamics simulations. Corresponding theoretical predictions are obtained within the analytical framework, previously developed for ferrofluid emulsions. The framework is proven to be accurate in the case when nanoparticles of the medium are immobilized. However, if particles are subjected to a translational Brownian motion, the applied field causes their local redistribution in the cluster vicinity. This behavior is reminiscent of the so-called “haloing” effect previously observed experimentally in bimodal magnetorheological fluids. It is shown that the haloing can lead to an anomalous increase of the system magnetization at large enough applied fields.

I. INTRODUCTION

Magnetic soft matter is a family of artificially synthesized materials based on a distributed system of magnetic particles embedded in a non-magnetic carrier matrix. Notable members of the said family are ferrofluids [1], magnetorheological fluids [2], ferrogels [3] and magnetoactive elastomers [4]. The behavior and properties of these systems can be controlled using applied magnetic fields, which makes them highly attractive in various branches of nanotechnology and nanomedicine. Examples of applications include soft crawling robots [5], tissue engineering scaffolds [6], adaptive dampers and seals [7], ferrofluid cooling systems [8], magnetic lubricants [9], targeted drug delivery systems [10], magnetic hyperthermia of cancers [11] and magnetic particle imaging [12].

Modern methods of magnetic soft matter synthesis have achieved a tremendous success. In particular, particles can vary greatly in size and can have very different internal magnetic structure. The common types of particles are single-domain ferro- or ferrimagnetic nanoparticles with linear sizes ~ 10 nm [13], dense cluster of single-domain nanocrystals (magnetic “nanoflowers” [14] and “multicore nanoparticles” [15, 16] with the size of the order of $\sim 10^2$ nm) and multi-domain microparticles with low or high coercivity [17]. Recently, multicomponent systems, which simultaneously employ several types of magnetic particles, attracted a lot of scientific attention. One example are hybrid elastomers containing both magnetically soft and hard microparticles [18]. Reportedly, they allow for a much larger degree of a magneto-mechanical fine-tuning than analogous one-component systems [19]. Bimodal magnetorheological fluids consist

of magnetic microparticles submerged in a nanodispersed ferrofluid [20]. They are considered to be an improved substitution for conventional magnetorheological fluids due to their superior colloidal stability and sedimentation behavior [21–23]. Even some samples of traditional ferrofluids are known to contain a fraction of nanoclusters, which results in a substantial alteration of their magnetic, mass-transport and rheological properties [24–26].

The creation of novel types of soft magnetic composites inevitably creates a demand for new theoretical approaches that can reliably build a connection between the material internal microstructure and its macroscopic magnetic response. Going forward, we will concentrate on composites based on single-domain fine particles. It is known that if the internal anisotropy energy of such particles is comparable or smaller than the energy of thermal fluctuations (which is common for iron oxide nanoparticles [13]), then the average ensemble magnetization in zero field will also be zero. As the field increases, the magnetization will non-linearly and reversibly grow towards the saturation value. Such behaviour is known as “superparamagnetism” and corresponding materials can be referred to as “superparamagnetic” [27]. In the last decades, many sophisticated theories were developed explaining magnetization of both liquid [28–30] and solid [31, 32] superparamagnets with a high content of magnetic nanoparticles and large energies of interparticle interactions. The majority of these theories are designed for a one-component system. A notable exception is the magnetostatic response theory for ferrofluid emulsions developed in Refs. [33–35]. Both direct and inverse ferrofluid emulsions are binary systems with only one magnetic component [36]. However, the general framework proposed in Refs. [34, 35] can potentially be applied for more complex cases with two superparamagnetic components. The viability and limitations of such approach is the central point of the present investigation.

* University of Vienna, Faculty of Physics, Computational and Soft Matter Physics, Kolingasse 14-16, 1090 Vienna, Austria.; andrey.kuznetsov@univie.ac.at

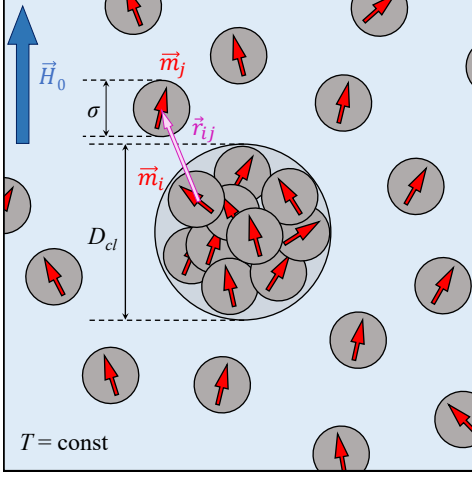


FIG. 1. Schematic representation of the investigated system

II. PROBLEM STATEMENT

A. Model of a binary superparamagnetic mixture

The system under consideration is a single magnetic nanocluster (or a “multicore nanoparticle” [16]) embedded in a superparamagnetic medium (see Figure 1). The system is subjected to an external uniform magnetic field H_0 and thermostated at a constant temperature T . Nanocluster is modelled as a sphere of diameter D_{cl} filled with N_{in} spherical magnetic particles of diameter σ . Particles are distributed within the cluster randomly and uniformly, without overlapping, their volume fraction is

$$\varphi_{in} = N_{in} \frac{(\pi/6)\sigma^3}{V_{cl}} = N_{in} \left(\frac{\sigma}{D_{cl}} \right)^3, \quad (1)$$

where $V_{cl} = \pi D_{cl}^3/6$ is the nanocluster volume. Positions of particles within the nanocluster are rigidly fixed. Particles are assumed to be single-domain and magnetically-isotropic. Each particle has a magnetic moment \vec{m} , which magnitude is fixed but whose orientation can change under the influence of an applied magnetic field, dipolar magnetic fields created by other magnetic moments in the system and thermal fluctuations. As a results, the nanocluster as a whole will have superparamagnetic properties. It does not have a net magnetic moment in the absence of an applied field, but will nonlinearly magnetize if the field is turned on [37]. The superparamagnetic medium surrounding the nanocluster is modelled in a similar fashion. It consists of N_{ex} magnetically-isotropic spherical single-domain particles, which are exactly the same as particles that constitute the cluster, i.e. they also have diameter σ and magnetic moment \vec{m} . The particle volume fraction in the medium is

$$\varphi_{ex} = N_{ex} \frac{(\pi/6)\sigma^3}{V_{tot} - V_{cl}}, \quad (2)$$

where V_{tot} is the total system volume. Magnetic nanoparticles in the medium always retain their rotational de-

grees of freedom. Regarding their translational movement, two cases will be separately considered. First of all, the “solid – solid” mixture (SSM). In this system, particles are randomly distributed in the medium and cannot move (just like particles in the nanocluster). Note that the ensemble of immobilized single-domain particles is often used as a toy model to study magnetic properties of some types of ferroelastomers [31]. The second case is the “solid – fluid” mixture (SFM). In this system, particles in the medium are subjected to a translational Brownian motion and can change their position relative to the cluster. They are assumed to be sterically stabilized and are not allowed to overlap.

The interaction of magnetic moments with the external field is governed by the Zeeman potential

$$U_Z = -\mu_0(\vec{m} \cdot \vec{H}_0), \quad (3)$$

where μ_0 is the magnetic permittivity of vacuum. Additionally, each pair of particles interacts via the magnetic dipole-dipole potential

$$U_{dd}(i, j) = \frac{\mu_0}{4\pi} \left[\frac{(\vec{m}_i \cdot \vec{m}_j)}{r_{ij}^3} - \frac{3(\vec{m}_i \cdot \vec{r}_{ij})(\vec{m}_j \cdot \vec{r}_{ij})}{r_{ij}^5} \right], \quad (4)$$

where \vec{m}_i and \vec{m}_j are magnetic moments of two particles and \vec{r}_{ij} is the vector connecting their centers. We use two dimensionless energy parameters to characterize these magnetic interactions. The first one is the Langevin parameter

$$\xi_0 = \frac{\mu_0 m H_0}{k_B T}, \quad (5)$$

that is the ratio of the Zeeman energy to the thermal energy $k_B T$, k_B is the Boltzmann constant, $m = |\vec{m}_i|$. The second parameter is the so-called dipolar coupling constant

$$\lambda = \frac{\mu_0}{4\pi} \frac{m^2}{\sigma^3 k_B T}, \quad (6)$$

that is the energy of two adjacent particles whose dipoles are aligned head-to-tail divided by $k_B T$.

Our main quantities of interest in this work are the normalized equilibrium magnetic moment of the nanocluster

$$\vec{\mathcal{M}}_{cl} = \left\langle \sum_{i=1}^{N_{in}} \vec{m}_i \right\rangle \frac{1}{m N_{in}}, \quad (7)$$

as well as the total normalized magnetic moment of the whole system

$$\vec{\mathcal{M}}_{tot} = \left\langle \sum_{i=1}^{N_{tot}} \vec{m}_i \right\rangle \frac{1}{m N_{tot}}, \quad (8)$$

where $N_{tot} = N_{in} + N_{ex}$ is the total number of particles, $\langle \dots \rangle$ denotes ensemble average.

In this work, Langevin dynamics simulations will be used as a main investigation tool. All technical details of simulations are given in the Appendix. However, it is important to specify that the system in simulations is subjected to 3D periodic boundary conditions. It approximately corresponds to a suspension of nanoclusters with a nanocluster volume fraction

$$\Phi_{cl} = \frac{V_{cl}}{V_{tot}} = \left(1 + \frac{\varphi_{in}}{\varphi_{ex}} \frac{N_{ex}}{N_{in}}\right)^{-1}. \quad (9)$$

We will consider systems with $N_{in} = 500$ and $N_{ex} = 2500$. Particle concentration in the cluster is always $\varphi_{in} = 0.3$, while the concentration of the surrounding medium will be changed from a small value of $\varphi_{ex} = 0.002$ to $\varphi_{ex} = 0.15$. Correspondingly, the cluster concentration will change from $\Phi_{cl} \simeq 0.0013$ to $\Phi_{cl} \simeq 0.09$. Magnetic interaction parameters also will vary in wide ranges: $1 \leq \lambda \leq 5$, $0 \leq \xi_0 \leq 5$.

B. Magnetic response theory

In addition to numerical simulations, we will also make an attempt to describe equilibrium magnetization of investigated systems analytically. We will use the works of Subbotin on inverse ferroemulsions as a basis of our consideration [34, 35]. Let us apply the theory to a suspension of spherical magnetizable bodies (clusters) in a magnetizable medium with a relative magnetic permeability μ_{ex} . Assume that the volume fraction of clusters is Φ_{cl} and they are made of some material with relative magnetic permeability μ_{in} . According to Refs. [34, 35], the field inside clusters is homogeneous and parallel to the external field, its magnitude is given by

$$H_{in} = H_0 \frac{1}{1 + (1 - \Phi_{cl})\kappa \left(\frac{\mu_{in}}{\mu_{ex}} - 1\right)}, \quad (10)$$

where κ is the cluster demagnetization factor. For a sphere, $\kappa = 1/3$. The field in the surrounding medium is

$$H_{ex} = H_0 \left[1 + \frac{\Phi_{cl}\kappa \left(\frac{\mu_{in}}{\mu_{ex}} - 1\right)}{1 + (1 - \Phi_{cl})\kappa \left(\frac{\mu_{in}}{\mu_{ex}} - 1\right)}\right]. \quad (11)$$

Permeabilities in general can be considered as non-linear functions of the field:

$$\mu_{in} = 1 + \frac{M_{in}(H_{in})}{H_{in}}, \quad (12)$$

$$\mu_{ex} = 1 + \frac{M_{ex}(H_{ex})}{H_{ex}}, \quad (13)$$

where M_{in} and M_{ex} are magnetizations of the cluster material and of the medium, respectively. The total magnetization of the system is

$$M_{tot} = \Phi_{cl}M_{in}(H_{in}) + (1 - \Phi_{cl})M_{ex}(H_{ex}). \quad (14)$$

Normalized magnetic moments then can be found as

$$\mathcal{M}_{cl} = \frac{M_{in}V_{cl}}{mN_{in}}, \quad 0 \leq \mathcal{M}_{cl} \leq 1, \quad (15)$$

$$\mathcal{M}_{tot} = \frac{M_{tot}V_{tot}}{mN_{tot}}, \quad 0 \leq \mathcal{M}_{tot} \leq 1. \quad (16)$$

Further on, the set of equations (10)–(16) will be referred to as the *binary mixture magnetization* (BMM) model.

The key assumption of BMM is that magnetic field in the medium H_{ex} is a sum of the external field H_0 and some average field that is created by all magnetized clusters distributed in the system. This latter field is assumed to be uniform and so is H_{ex} itself. However, it is known that the local magnetic field (and subsequently μ_{ex}) in the vicinity of a magnetized spherical body is non-uniform [13]. Thus, Eqs. (10)–(11) are only an approximation. BMM, however, converges to a well-known Maxwell-Wagner formula for the initial permeability of a binary dielectric mixture [38]. In the weak-field limit, it also shows a good agreement with experimental data on the effective permeability of inverse ferroemulsions. But as the applied field increases, it overestimates experimental results slightly. Applicability of BMM to our system is to be determined.

In order to close the set of BMM equations, some explicit expressions for magnetization curves $M_{in} = M_{in}(H_{in})$ and $M_{ex} = M_{ex}(H_{ex})$ are required. For this purpose, the so-called *modified mean-field* (MMF) theory can be used. It was initially developed to describe static magnetic properties of concentrated ferrofluids [28, 39]. Subsequently, the approach has been extended for the description of the ferrofluid dynamic response [40] as well as magnetic properties of single-domain nanoparticle ensembles immobilized in a solid non-magnetic matrix [31]. Ref. [35] used MMF as well. Within MMF (more specifically, within the second order version of MMF), magnetization of a one-component superparamagnetic material is

$$M(H) = M_s L \left(\xi_{eff} \left(\frac{\mu_0 m H}{k_B T}, \chi_L \right) \right), \quad (17)$$

$$\xi_{eff}(\xi, \chi_L) = \xi + \chi_L (1 + \chi_L L'(\xi)/16) L(\xi), \quad (18)$$

$$L(\xi) = \coth \xi - 1/\xi, \quad (19)$$

where $M_s = (6/\pi\sigma^3)m\varphi$ is the medium saturation magnetization, φ is the particle volume fraction within this medium, $\chi_L = 8\lambda\varphi$ is the so-called Langevin susceptibility, $L(\xi)$ is the Langevin function that describes magnetic response of an ensemble of non-interacting dipoles (i.e., at $\chi_L \ll 1$), $L'(\xi) = dL(\xi)/d\xi$, ξ_{eff} is the effective dimensionless field that is acting on an arbitrary particle in an ensemble with dipole-dipole interactions. If we assume that components of our binary mixture both can be described by MMF, permeabilities can be written down

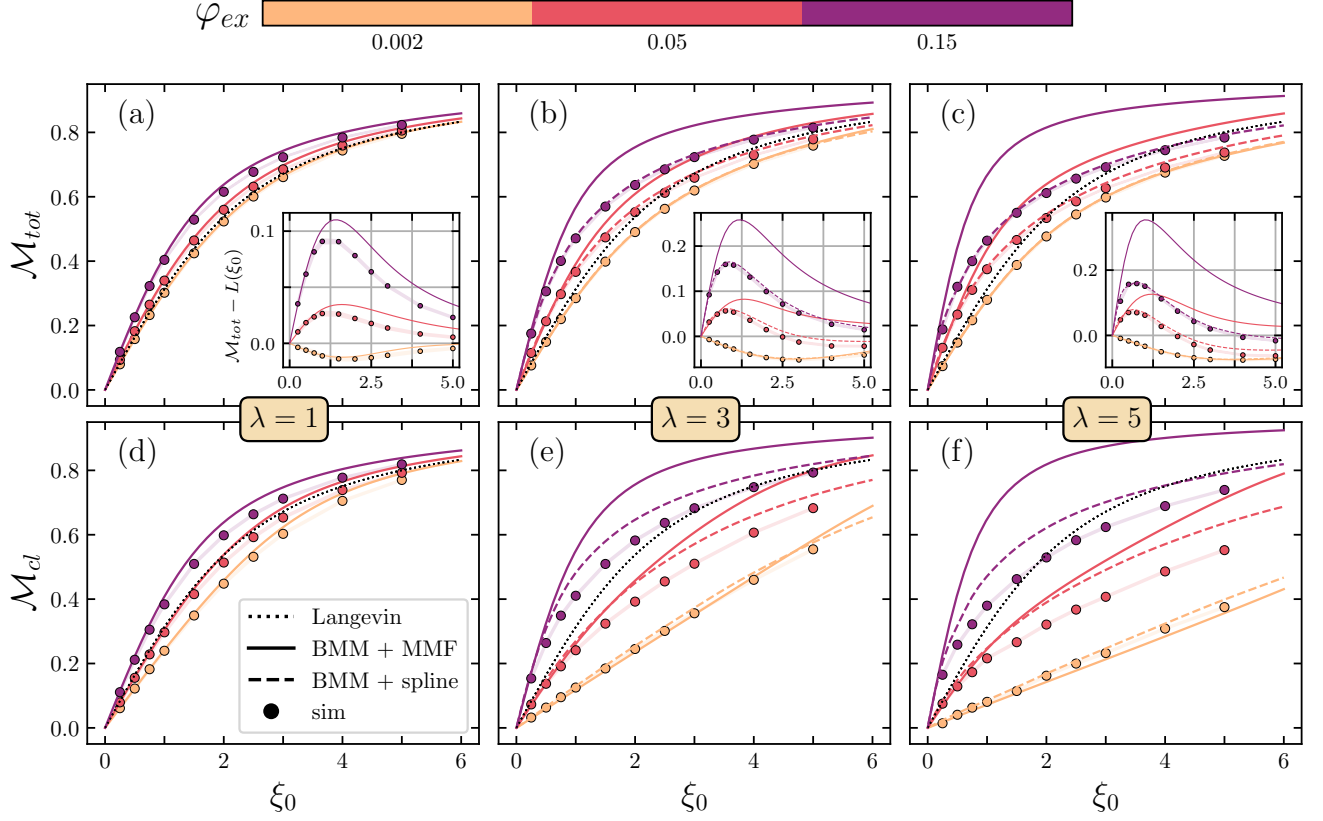


FIG. 2. Equilibrium magnetization curves for a “solid-solid” superparamagnetic mixture. The first row (panels (a)–(c)) demonstrates dependencies of a normalized magnetization (or, identically, of a normalized magnetic moment) of the whole system \mathcal{M}_{tot} on the Langevin parameter ξ_0 . Insets in (a)–(c) shows the difference between \mathcal{M}_{tot} values from the corresponding panels and the applied field Langevin function. The latter is indicated on the main panels with **dotted lines**. The second row (panels (d)–(f)) shows corresponding values of the cluster normalized magnetic moment \mathcal{M}_{cl} . Different columns correspond to different dipolar coupling parameters: (a), (d) $\lambda = 1$; (b), (e) $\lambda = 3$; (c), (f) $\lambda = 5$. Particle volume fraction in the surrounding medium φ_{ex} is indicated by color (see colorbar). Simulation results are shown with **circles**, **solid lines** are predictions from BMM model [Eqs. (10)–(16)] combined with MMF expressions for magnetic permeabilities [Eqs. (20)–(21)]. **Dashed lines** are “corrected” BMM predictions with permeabilities values extracted from auxiliary simulations of one-component superparamagnetic systems (see text).

as

$$\mu_{in} = 1 + 3\chi_L^{in} \frac{L(\xi_{eff}(\xi_{in}, \chi_L^{in}))}{\xi_{in}}, \quad (20)$$

$$\mu_{ex} = 1 + 3\chi_L^{ex} \frac{L(\xi_{eff}(\xi_{ex}, \chi_L^{ex}))}{\xi_{ex}}, \quad (21)$$

where $\chi_L^{in} = 8\lambda\varphi_{in}$, $\chi_L^{ex} = 8\lambda\varphi_{ex}$, $\xi_{in} = \mu_0 m H_{in} / k_B T$, $\xi_{ex} = \mu_0 m H_{ex} / k_B T$.

III. RESULTS AND DISCUSSION

A. Equilibrium magnetization of a solid-solid mixture

Magnetization curves for a superparamagnetic cluster embedded in a solid matrix with immobilized nanoparticles are shown in Figure 2 for different values of λ and

φ_{ex} . The first noticeable feature of magnetization curves is that at any given λ an increase in φ_{ex} leads to a qualitative change in how the system magnetization relates to a Langevin function. Langevin magnetization corresponds to a system of non-interacting dipoles. So, if the normalized magnetization is lower than corresponding Langevin value, it means that dipole-dipole interactions decrease overall magnetic response. Vice versa, magnetization higher than the Langevin value indicates that dipole-dipole interactions play a reinforcing role. It is known that equilibrium magnetostatic response of superparamagnetic clusters in an empty space always lies below the Langevin curve [37] – this is the result of the demagnetization effect. Similar behavior is observed in our system for cluster in a diluted medium with $\varphi_{ex} = 0.002$. However, as the concentration of particles in the surrounding medium increases (and as the magnetic permeability of the medium μ_{ex} becomes closer to the permeability of the cluster μ_{in}), demagnetization effect slowly disappears –

magnetization of both the cluster and the mixture eventually becomes larger than the Langevin value. Interestingly enough, at $\varphi_{ex} \geq 0.05$ and $\lambda \geq 3$ the effect of dipole-dipole interactions on the mixture magnetization depends non-monotonically on the field – while the initial section of the magnetization curve is larger than that of the Langevin function, simulation points eventually fall below $L(\xi)$ in the saturation regime.

As for the theoretical predictions, it is seen that the combination of BMM and MFT gives very accurate predictions for the initial slope of magnetization curves in the whole investigated parameter ranges. However, as the field increases, theory and simulation data start to diverge rapidly. The larger φ_{ex} and/or λ the stronger the discrepancy. Theoretical curves are always above simulation points at $\xi_0 > 1$. At $\varphi_{ex} = 0.15$ and $\lambda = 5$, the error between numerical and theoretical values of the mixture magnetization reaches almost 20% of the corresponding saturation value.

To understand the reason for the discrepancy between theory and simulations, a set of auxiliary simulations was performed. We simulated a one-component ensemble of immobilized nanoparticles randomly and uniformly distributed in a standard cubic box with 3D periodic boundary conditions. Ensemble of $N = 2000$ particles was considered. Using simulation data, a non-linear magnetic permeability of the ensemble was calculated as a function of the field ξ at different λ and particle volume fractions φ . The results are demonstrated in Figure 3 in comparison with MMF predictions. It can be seen that while MMF mostly predicts correct zero-field permeability values, at large fields it overestimates μ . In more details this feature of immobilized superparamagnetic ensembles was discussed in Ref. [37]. To take it into account the following procedure was performed. Calculated permeability of a one-component system were interpolated (with cubic splines) and then put in BMM instead of MMF predictions Eqs. (20) and (21). The results of this procedure are shown in Figure 2 with dashed lines. We can see that the accuracy of BMM with “corrected” permeabilities improves drastically. New theoretical curves closely follow \mathcal{M}_{tot} dependencies. The magnetization curves for the cluster still overestimate numerical results but it is much better than MMF for $\lambda \geq 3$ and $\varphi_{ex} \geq 0.05$. The probable reason for the remaining discrepancy is the inherent BMM assumption that the magnetic field H_{ex} and permeability of the surrounding medium μ_{ex} are constant and uniform in cluster vicinity, which is not correct at large enough applied fields [13]. Thus, the agreement with simulation potentially can only be improved by directly solving a nonlinear magnetostatic boundary-value problem and correctly determining the magnetic field distribution in the system. However, this task is beyond the scope of the present paper.

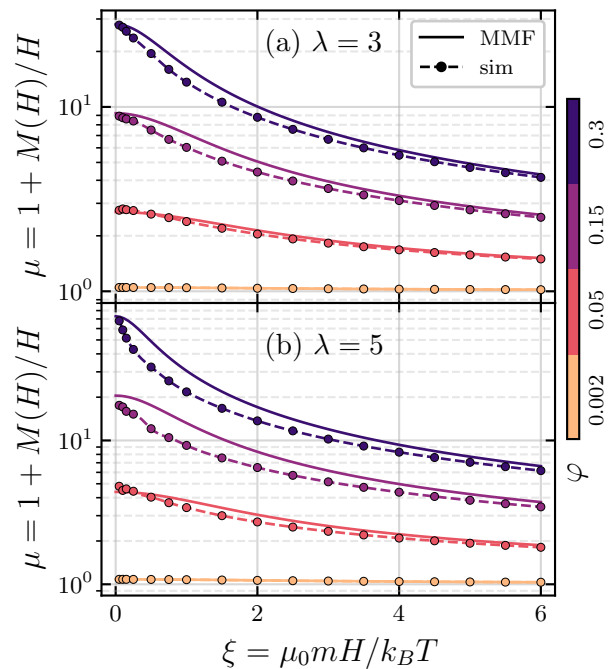


FIG. 3. Field dependencies of the magnetic permeability for a one-component ensemble of randomly distributed immobilized magnetic nanoparticles. **Solid lines** are MMF theory predictions [Eqs. (17)-(18)], **symbols** are simulation results. Different panels correspond to different dipolar coupling constants: $\lambda = 3$ (a) and 5 (b). Particle volume fractions are indicated by color.

B. Equilibrium magnetization of a solid-fluid mixture

Now let us consider a different type of a binary mixture – a superparamagnetic nanocluster submerged in a suspension of magnetic nanoparticles in a non-magnetic liquid matrix. Essentially, a nanocluster in a ferrofluid. The magnetization curves for this case are shown in Figure 4. The first thing that is seen here is that the magnetization of the mixture and the cluster are larger than corresponding SSM values for every set of investigated parameters. A noticeable feature of SSM at large φ_{ex} is that \mathcal{M}_{tot} can be larger than the corresponding Langevin value in weak fields, but smaller than the Langevin value in large fields. For SFM this feature is no longer present – at least not at $\xi_0 \leq 5$.

MMF does not make any distinctions between liquid and solid superparamagnetic ensembles – thus, theoretical curves in Figure 4 are exactly the same as in Figure 2. At $\lambda = 1$, these curves actually describe simulation data for a solid-fluid mixture quite well – better than the data for a solid-solid one. But already at $\lambda = 3$ the agreement breaks down. Surprisingly, the error does not increase with φ_{ex} as in SSM case – the strongest disagreement between theory and simulations takes place at the intermediate concentration. For $\lambda = 3$ and $\varphi_{ex} = 0.05$,

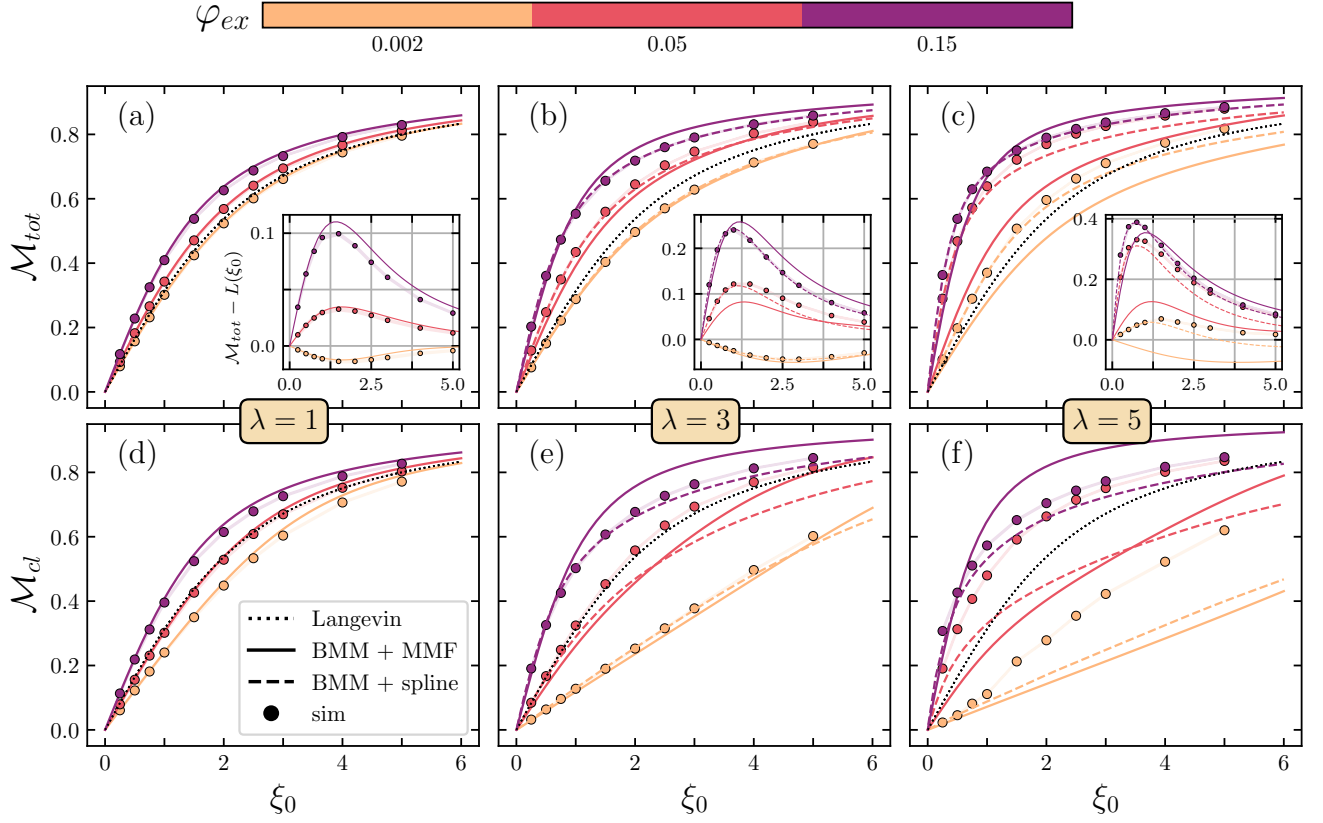


FIG. 4. Equilibrium magnetization curves for a “solid–fluid” superparamagnetic mixture. The notation is identical to Figure 2.

theoretical predictions are incorrect both for initial and saturation portions of the SFM magnetization curve. At $\lambda = 5$ the strongest disagreement takes place at even smaller concentrations – at $\varphi_{ex} = 0.002$.

In order to improve the agreement, the same procedure was employed as for SSM. Namely, an auxiliary set of simulations of a one-component superparamagnetic system was performed. This time, the one-component system is a liquid suspension of single-domain particles. The results for a non-linear magnetic permeability of this systems at different particle concentrations and dipolar coupling constants are given in Figure 5. Comparing it with Figure 3, we can see that the relation between actual permeability and MMF predictions for liquid and solid one-component superparamagnets is completely opposite. For solid systems, MMF gives correct zero-field values, but overestimates numerical results as the field increases. For a liquid, zero-field permeabilities are much larger than MMF predictions but in large fields the agreement is almost perfect. This zero-field behaviour is actually a well-known phenomenon that is attributed to the formations of particle chains in a ferrofluid with strong dipolar interactions [41]. Once again, numerically obtained permeability curves were interpolated with cubic splines and then used within BMM approach instead of MMF predictions Eqs. (20) and (21). The results of this correction are shown in Figure 4 with dashed lines. Un-

fortunately, the correction no longer gives the same accuracy boost as for SSM. In fact, it only improves the initial slope of the magnetization curves. But at large fields, simulation results lie way above the predictions of the corrected BMM. It is most clearly demonstrated by \mathcal{M}_{tot} and \mathcal{M}_{cl} dependencies for $\lambda = 5$ and $\varphi_{ex} = 0.002$.

So, it can be deduced that some qualitative change is happening in SMF system as the field increases. It leads to a significant increase of normalized magnetic moments \mathcal{M}_{tot} and \mathcal{M}_{cl} , which cannot be explained within BMM approach. This phenomenon is more pronounced at large λ and smaller φ_{ex} . It does not take place in SSM. To get a better understanding of what is happening here, a deeper analysis of the system microstructure can be useful.

C. Field-controlled haloing in a solid-fluid mixture

Let us look closely on the behavior of the simulated SFM system at $\lambda = 5$ and $\varphi_{ex} = 0.002$ – i.e., in the parameter ranges, in which deviations from theoretical magnetization curves are most pronounced. Corresponding simulation snapshots are given in Figure 6 for different strength values of the applied field. At a relatively small field with $\xi_0 = 1$ free nanoparticles form chain-like structures, as is expected at $\lambda = 5$ [41]. The presence of a cluster does not produce any clearly visible effects on

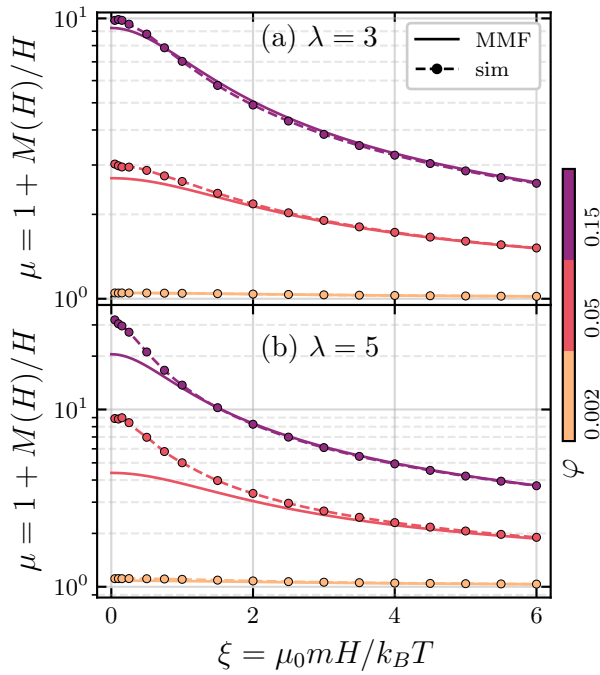


FIG. 5. Field dependencies of the magnetic permeability for a one-component ensemble of magnetic nanoparticles suspended in a liquid matrix (i.e., particles are subjected to a translational Brownian motion). The notation is identical to Figure 3.

the system microstructure. However, already at $\xi_0 = 2$ and especially at $\xi_0 = 4$ a significant change takes place – particles (or rather, particle chains) start to concentrate near the nanocluster poles forming concentrated clouds stretched along the field direction. This phenomena is qualitatively reminiscent of the so-called “haloing” effect, experimentally observed in bimodal magnetorheological fluids [20, 42]. The only difference is that in the latter systems superparamagnetic nanoclusters form thick clouds (or “halos”) around magnetizable microparticles. The physical reason behind this halo formation is the phenomenon of magnetophoresis – i.e., the movement of magnetic nanoparticles in a gradient magnetic field [25, 43]. The source of the inhomogeneous field in our case is the magnetized nanocluster [13]. The stronger the applied field, the stronger the cluster’s own field gradient. This gradient is directed towards poles of the cluster, where free nanoparticles tend to accumulate.

It is known that the transport of magnetic nanoparticles in a viscous medium is affected strongly by interparticle interactions [44, 45]. Namely, dipole-dipole interactions controlled by λ are acting as effective attraction between particles. They effectively decrease the gradient diffusion coefficient of the system and make it much easier to create a strongly inhomogeneous particle distribution with a given applied field. The effect of dipole-dipole interactions on particle transport is typically most pronounced at intermediate average concentrations $\varphi \leq 0.1$.

In more dense systems, the steric repulsion (i.e., the excluded volume effect) starts to dominate and substantially increases the gradient diffusion coefficient. In other words, it is hard to create a noticeable concentration gradient in a highly concentrated system. All these theoretical considerations are well illustrated and validated by SFM concentration maps shown in Figure 7. First, halos concentration increases with λ . At $\varphi_{ex} = 0.002$ and $\lambda = 5$, the *local* concentration of particles near cluster poles is actually comparable with the cluster concentration itself ($\varphi_{in} = 0.3$) and two order of magnitude larger than near the cluster “flanks”. Thus, the situation can be interpreted as follows – the cluster, which is spherical in small fields, start to “grow” with increasing ξ_0 and turns into an elongated particle aggregate aligned with the field. As the aggregate shape changes, its demagnetization factor [κ in Eqs. (10)-(11)] decreases. It is very similar to the behavior of magnetic droplets in ferroemulsions [33] and can explain the anomalous increase of the cluster magnetization seen in Figure (4)(f). The haloing is still present at larger average concentrations. But important difference is that at higher average volume fractions the inhomogeneity of the local concentration decreases. In the most dense environment with the average particle concentration $\varphi_{ex} = 0.15$, the local particle concentration near cluster surface is always $\varphi_{ex,loc} \geq 0.1$. As the result, BMM (which assumes the system homogeneity) still works relatively well for this case.

IV. CONCLUSIONS

In this work, equilibrium magnetic response of a binary superparamagnetic mixture is studied both theoretically and numerically (with the help of Langevin dynamic simulations). One component of the mixture is a quasispherical nanocluster consisting of immobilized magneto-isotropic single-domain particles. The cluster is submerged in a superparamagnetic medium, which itself constitutes an ensemble of single-domain particles in a non-magnetic matrix. Two cases are separately considered. In the first case (SSM), particles of the surrounding medium are spatially immobilized, although they fully retain rotational degrees of freedom. This case is a simplification, which allows us to neglect possible effects of Brownian motion and self-aggregation. In the second case (SFM), particles in the medium have both translation and rotational degrees of freedom. It is shown that magnetostatic response of the SSM system can be accurately described theoretically within BMM approach [Eqs. (10)-(16)], if the non-linear permeabilities of individual mixture components are known. It is also shown that MMF predictions for permeabilities [Eqs. (20)-(21)] give accurate description of the simulation data only at relatively small values of the dipolar coupling constant ($\lambda \leq 1$). The situation changes qualitatively for SFM system. If the average particle concentration in the medium is low

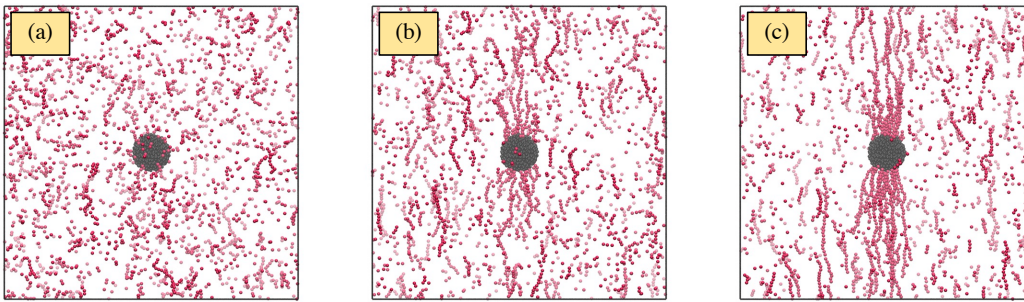


FIG. 6. Simulation snapshots of the “solid–fluid” mixture at $\varphi_{ex} = 0.002$ and $\lambda = 5$. Different panels correspond to different Langevin parameters: $\xi_0 = 1$ (a), 2 (b) and 4 (c). Applied field is oriented vertically.

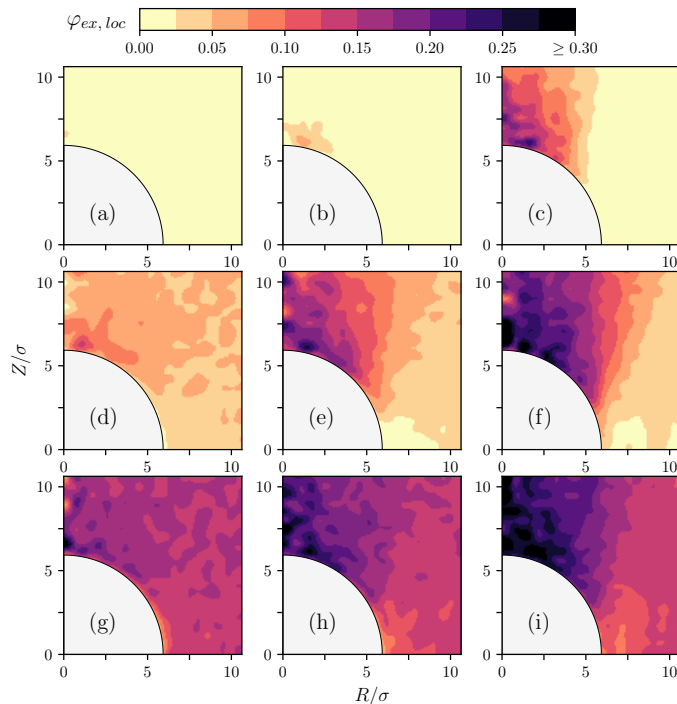


FIG. 7. Local particle volume fraction $\varphi_{ex,loc}$ in the vicinity of the cluster. Numerical values of $\varphi_{ex,loc}$ are indicated by the color (see colorbar), the cluster is colored grey. Maps are constructed using space- and time-averaged data from 3D Langevin dynamics simulation. They are plotted in a cylindrical coordinates (R, Z) with the origin at the cluster center. Only the upper right corner is shown due to the system symmetry. Langevin parameter is $\xi_0 = 3$, the field is directed along Z axis. Dipolar coupling constant is increasing from left to right: (a),(d),(g) $\lambda = 1$; (b),(e),(h) $\lambda = 3$; (c),(f),(i) $\lambda = 5$. The *average* volume fraction of particles is increasing from top to bottom: (a)–(c) $\varphi_{ex} = 0.002$; (d)–(f) $\varphi_{ex} = 0.05$; (g)–(i) $\varphi_{ex} = 0.15$.

enough, magnetization of the mixture grows anomalously fast with the field (compared to BMM prediction). The apparent reason for this growth is the so-called haloing effect: the gradient field of the magnetized nanocluster leads to the local redistribution of particles in the surrounding medium. It is shown that particles form concentrated clouds near the cluster poles, which decreases demagnetization effect within its volume and makes it more susceptible to the applied field. A strong dependence of the haloing effect on the intensity of dipole-dipole inter-

actions is revealed.

We can conclude that an accurate theoretical description of the magnetostatic response of a binary superparamagnetic mixture at $\lambda > 1$ cannot simply assume the spatial homogeneity of the systems’s magnetic properties. The local inhomogeneity of the cluster field and the subsequent drift-diffusion particle transport must be explicitly taken into account. In practice, it will require the solution of a combined magneto-diffusive boundary value problem, similar to those previously considered in

Refs. [46, 47]. The solution of this problem is left for future studies.

CONFLICTS OF INTEREST

There are no conflicts to declare.

ACKNOWLEDGEMENTS

The study was funded by RFBR, project number 19-31-60036. All computations were performed at the Ural Federal University cluster. Partial support from FWF Project SAM P 33748 is also acknowledged.

APPENDIX: SIMULATION DETAILS

In a numerical realization of our mixture model, we consider a cubic simulation box with length $l = V_{tot}^{1/3}$. The cluster is placed in the center of this box. Its position does not change during the simulation. 3D periodic boundary conditions are imposed on a box. The field is directed along Z -axis. All the results reported are obtained using ESPResSo 4.1 simulation package [48].

Rotational motion of the i -th particle is governed by the Langevin equation

$$J^* \frac{d\vec{\omega}_i^*}{dt^*} = \vec{\tau}_i^* - \gamma^{*R} \vec{\omega}_i^* + \vec{\eta}_i^{*R}, \quad \frac{d\vec{m}_i}{dt^*} = \vec{\omega}_i^* \times \vec{m}_i, \quad (22)$$

For SFM, translational motion of the i -th particle in a medium is additionally described by an analogous equation

$$\frac{d\vec{v}_i^*}{dt^*} = \vec{f}_i^* - \gamma^{*T} \vec{v}_i^* + \vec{\eta}_i^{*T}. \quad (23)$$

Here asterisk denotes reduced quantities, σ is used as a unit of length, particle mass u – as a unit of mass and the thermal energy $k_B T$ – as a unit of energy. Thus, $\vec{v}_i^* = \vec{v}_i \sqrt{u/k_B T}$ and $\vec{\omega}_i^* = \vec{\omega}_i \sqrt{u\sigma^2/k_B T}$ are

the reduced linear and angular velocities, correspondingly, $J^* = J/ud^2$ is the reduced moment of inertia, $\gamma^{*T} = \gamma^T \sqrt{\sigma^2/uk_B T}$ and $\gamma^{*R} = \gamma^R \sqrt{1/\sigma^2 uk_B T}$ are the reduced translational and rotational friction coefficients, $\vec{\eta}_i^{*R}$ and $\vec{\eta}_i^{*T}$ are the random force and torque, which have zero mean values and satisfy the standard fluctuation-dissipation relationship [49]

$$\langle \eta_{i\alpha}^{*T(R)}(t_1^*) \eta_{j\beta}^{*T(R)}(t_2^*) \rangle = 2\gamma^{*T(R)} \delta_{\alpha\beta} \delta_{ij} \delta^*(t_1^* - t_2^*), \quad (24)$$

α and β denote Cartesian vector components, $\delta^*(t^*)$ is the Dirac delta function, δ_{ij} is the Kronecker delta, the reduced time is $t^* = t\sqrt{k_B T/u\sigma^2}$. $\vec{\tau}_i^* = \mu_0 [\vec{m}_i \times (\vec{H}_0 + \vec{H}_{dd}(i))] / k_B T$ is the reduced magnetic torque acting on a given particle, $\vec{H}_{dd}(i) = -(1/\mu_0) \sum_{j \neq i} \partial U_{dd}(i, j) / \partial \vec{m}_i$ is the sum all dipolar fields in the particle center, $\vec{f}_i^* = -(\sigma/k_B T) \sum_{j \neq i} \partial (U_{dd}(i, j) + U_{WCA}(i, j)) / \partial \vec{r}_i$ is the total reduced force on the particle, $U_{WCA}(i, j)$ is the Weeks-Chandler-Andersen (WCA) pair potential that simulates steric repulsion between particles [50]:

$$U_{WCA}(i, j) = \begin{cases} U_{LJ}(r_{ij}) - U_{LJ}(r_{cut}), & r_{ij} < r_{cut} \\ 0, & r_{ij} \geq r_{cut}, \end{cases} \quad (25)$$

$$U_{LJ}(r) = 4\epsilon \left[\left(\frac{\sigma}{r} \right)^{12} - \left(\frac{\sigma}{r} \right)^6 \right], \quad (26)$$

where U_{LJ} is the Lennard-Jones potential, $r_{cut} = 2^{1/6} \sigma$.

Note that if one is interested in a rigorous investigation of the system non-equilibrium properties, then the stochastic Landau-Lifshitz-Gilbert equation [37, 51] is more preferable for the rotational dynamics of particles' magnetic moments than Eq. (22). However, here we are only interested in a magnetostatic response and Eq. (22) is capable of producing the correct equilibrium distribution of magnetic moments.

The forces and torques due to long-range dipole-dipole interactions are computed using the dipolar P³M algorithm with “metallic” boundary conditions [52]. All the results are reported for $J^* = \gamma_R^* = \gamma_T^* = \epsilon^* = 1$, simulation time step is $\Delta t^* = 0.01$.

-
- [1] M. I. Shliomis, Magnetic fluids, *Phys. Usp.* **17**, 153 (1974).
 - [2] G. Bossis, S. Lacis, A. Meunier, and O. Volkova, Magnetorheological fluids, *Journal of magnetism and magnetic materials* **252**, 224 (2002).
 - [3] R. Weeber, M. Hermes, A. M. Schmidt, and C. Holm, Polymer architecture of magnetic gels: a review, *Journal of Physics: Condensed Matter* **30**, 063002 (2018).
 - [4] C. Bellan and G. Bossis, Field dependence of viscoelastic properties of mr elastomers, *International journal of modern physics B* **16**, 2447 (2002).
 - [5] K. Zimmermann, V. Naletova, I. Zeidis, V. Böhm, and E. Kolev, Modelling of locomotion systems using deformable magnetizable media, *Journal of Physics: Condensed Matter* **18**, S2973 (2006).
 - [6] N. Bock, A. Riminucci, C. Dionigi, A. Russo, A. Tampieri, E. Landi, V. A. Goranov, M. Marcacci, and V. Dediu, A novel route in bone tissue engineering: magnetic biomimetic scaffolds, *Acta Biomaterialia* **6**, 786 (2010).
 - [7] S. Abramchuk, E. Kramarenko, D. Grishin, G. Stepanov, L. Nikitin, G. Filipcsei, A. Khokhlov, and M. Zrínyi,

- Novel highly elastic magnetic materials for dampers and seals: part ii. material behavior in a magnetic field, *Polymers for Advanced Technologies* **18**, 513 (2007).
- [8] W. Cherief, Y. Avenas, S. Ferrouillat, A. Kedous-Lebouch, L. Jossic, and M. Petit, Parameters affecting forced convection enhancement in ferrofluid cooling systems, *Applied Thermal Engineering* **123**, 156 (2017).
 - [9] W. Huang, C. Shen, S. Liao, and X. Wang, Study on the ferrofluid lubrication with an external magnetic field, *Tribology Letters* **41**, 145 (2011).
 - [10] R. Tietze, S. Lyer, S. Dürr, T. Struffert, T. Engelhorn, M. Schwarz, E. Eckert, T. Göen, S. Vasylyev, W. Peukert, *et al.*, Efficient drug-delivery using magnetic nanoparticles—biodistribution and therapeutic effects in tumour bearing rabbits, *Nanomedicine: Nanotechnology, Biology and Medicine* **9**, 961 (2013).
 - [11] E. A. Périgo, G. Hemery, O. Sandre, D. Ortega, E. Garaio, F. Plazaola, and F. J. Teran, Fundamentals and advances in magnetic hyperthermia, *Applied Physics Reviews* **2**, 041302 (2015).
 - [12] Z. W. Tay, P. Chandrasekharan, A. Chiu-Lam, D. W. Hensley, R. Dhavalikar, X. Y. Zhou, E. Y. Yu, P. W. Goodwill, B. Zheng, C. Rinaldi, *et al.*, Magnetic particle imaging-guided heating in vivo using gradient fields for arbitrary localization of magnetic hyperthermia therapy, *ACS nano* **12**, 3699 (2018).
 - [13] R. E. Rosensweig, *Ferrohydrodynamics* (Cambridge University Press, Cambridge, 1985).
 - [14] P. Bender, D. Honecker, and L. Fernández Barquín, Supraferromagnetic correlations in clusters of magnetic nanoflowers, *Applied Physics Letters* **115**, 132406 (2019).
 - [15] F. Ludwig, O. Kazakova, L. F. Barquín, A. Fornara, L. Trahms, U. Steinhoff, P. Svedlindh, E. Wetterskog, Q. A. Pankhurst, P. Southern, *et al.*, Magnetic, structural, and particle size analysis of single- and multi-core magnetic nanoparticles, *IEEE transactions on magnetics* **50**, 1 (2014).
 - [16] V. Socoliuc, M. Avdeev, V. Kuncser, R. Turcu, E. Tombácz, and L. Vekas, Ferrofluids and bio-ferrofluids: looking back and stepping forward, *Nanoscale* **14**, 4786 (2022).
 - [17] D. Borin, G. Stepanov, and E. Dohmen, Hybrid magnetoactive elastomer with a soft matrix and mixed powder, *Archive of Applied Mechanics* **89**, 105 (2019).
 - [18] P. A. Sánchez, O. V. Stolbov, S. S. Kantorovich, and Y. L. Raikher, Modeling the magnetostriction effect in elastomers with magnetically soft and hard particles, *Soft Matter* **15**, 7145 (2019).
 - [19] T. Becker, K. Zimmermann, D. Y. Borin, G. Stepanov, and P. Storozhenko, Dynamic response of a sensor element made of magnetic hybrid elastomer with controllable properties, *Journal of magnetism and magnetic materials* **449**, 77 (2018).
 - [20] C. Magnet, P. Kuzhir, G. Bossis, A. Meunier, L. Suloeva, and A. Zubarev, Haloing in bimodal magnetic colloids: The role of field-induced phase separation, *Phys. Rev. E* **86**, 011404 (2012).
 - [21] J. Viota, F. González-Caballero, J. Durán, and A. Delgado, Study of the colloidal stability of concentrated bimodal magnetic fluids, *Journal of colloid and interface science* **309**, 135 (2007).
 - [22] M. T. López-López, A. Y. Zubarev, and G. Bossis, Repulsive force between two attractive dipoles, mediated by nanoparticles inside a ferrofluid, *Soft Matter* **6**, 4346 (2010).
 - [23] R. Rosensweig, Magnetorheological particle clouds, *Journal of Magnetism and Magnetic Materials* **479**, 301 (2019).
 - [24] V. M. Buzmakov and A. F. Pshenichnikov, On the structure of microaggregates in magnetite colloids, *J. Colloid Interface Sci.* **182**, 63 (1996).
 - [25] A. F. Pshenichnikov and A. S. Ivanov, Magnetophoresis of particles and aggregates in concentrated magnetic fluids, *Phys. Rev. E* **86**, 051401 (2012).
 - [26] D. Borin, A. Zubarev, D. Chirikov, R. Müller, and S. Odenbach, Ferrofluid with clustered iron nanoparticles: Slow relaxation of rheological properties under joint action of shear flow and magnetic field, *J. Magn. Magn. Mater.* **323**, 1273 (2011).
 - [27] C. P. Bean and J. D. Livingston, Superparamagnetism, *J. Appl. Phys.* **30**, S120 (1959).
 - [28] A. O. Ivanov and O. B. Kuznetsova, Magnetic properties of dense ferrofluids: an influence of interparticle correlations, *Phys. Rev. E* **64**, 041405 (2001).
 - [29] B. Huke and M. Lücke, Magnetic properties of colloidal suspensions of interacting magnetic particles, *Rep. Prog. Phys.* **67**, 1731 (2004).
 - [30] A. O. Ivanov, S. S. Kantorovich, V. S. Zverev, E. A. Elfimova, A. V. Lebedev, and A. F. Pshenichnikov, Temperature-dependent dynamic correlations in suspensions of magnetic nanoparticles in a broad range of concentrations: a combined experimental and theoretical study, *Phys. Chem. Chem. Phys.* **18**, 18342 (2016).
 - [31] E. A. Elfimova, A. O. Ivanov, and P. J. Camp, Static magnetization of immobilized, weakly interacting, superparamagnetic nanoparticles, *Nanoscale* **11**, 21834 (2019).
 - [32] D. I. Radushnov, A. Y. Solovyova, and E. A. Elfimova, Structure and magnetization of a magnetoactive ferrocomposite, *Nanoscale* **14**, 10493 (2022).
 - [33] A. O. Ivanov and O. B. Kuznetsova, Nonmonotonic field-dependent magnetic permeability of a paramagnetic ferrofluid emulsion, *Phys. Rev. E* **85**, 041405 (2012).
 - [34] I. M. Subbotin, Magnetic permeability of inverse ferrofluid emulsion: an influence of interdroplet interaction, *Magnetohydrodynamics* **54**, 131 (2018).
 - [35] I. M. Subbotin, Magnetic permeability of inverse ferrofluid emulsion: Nonlinear ferrofluid magnetization law, *Journal of Magnetism and Magnetic Materials* **502**, 166524 (2020).
 - [36] A. Zakinyan and I. Arefyev, Thermal conductivity of emulsion with anisotropic microstructure induced by external field, *Colloid and Polymer Science* **298**, 1063 (2020).
 - [37] A. A. Kuznetsov, Equilibrium magnetization of a quasi-spherical cluster of single-domain particles, *Physical Review B* **98**, 144418 (2018).
 - [38] H. Fricke, The maxwell-wagner dispersion in a suspension of ellipsoids, *The Journal of Physical Chemistry* **57**, 934 (1953).
 - [39] A. F. Pshenichnikov, V. V. Mekhonoshin, and A. V. Lebedev, Magneto-granulometric analysis of concentrated ferrocolloids, *J. Magn. Magn. Mater.* **161**, 94 (1996).
 - [40] A. O. Ivanov, V. S. Zverev, and S. S. Kantorovich, Revealing the signature of dipolar interactions in dynamic spectra of polydisperse magnetic nanoparticles, *Soft matter* **12**, 3507 (2016).
 - [41] A. O. Ivanov, Z. Wang, and C. Holm, Applying the chain

- formation model to magnetic properties of aggregated ferrofluids, *Phys. Rev. E* **69**, 031206 (2004).
- [42] C. Magnet, P. Kuzhir, G. Bossis, A. Meunier, S. Nave, A. Zubarev, C. Lomenech, and V. Bashtovoi, Behavior of nanoparticle clouds around a magnetized microsphere under magnetic and flow fields, *Physical Review E* **89**, 032310 (2014).
 - [43] A. A. Kuznetsov and I. A. Podlesnykh, Magnetophoretic equilibrium of a polydisperse ferrofluid, *Nanomaterials* **11**, 2849 (2021).
 - [44] A. F. Pshenichnikov, E. A. Elfimova, and A. O. Ivanov, Magnetophoresis, sedimentation, and diffusion of particles in concentrated magnetic fluids, *J. Chem. Phys.* **134**, 184508 (2011).
 - [45] A. A. Kuznetsov and A. F. Pshenichnikov, Sedimentation equilibrium of magnetic nanoparticles with strong dipole-dipole interactions, *Phys. Rev. E* **95**, 032609 (2017).
 - [46] O. Lavrova, V. Polevikov, and L. Tobiska, Modeling and simulation of magnetic particles diffusion in a ferrofluid layer, *Magnetohydrodynamics* **52**, 417 (2016).
 - [47] O. Lavrova and V. Polevikov, Numerical study of the shielding properties of a ferrofluid taking into account magnetophoresis and particle interaction, *Mathematical Modelling and Analysis* **27**, 161 (2022).
 - [48] F. Weik, R. Weeber, K. Szuttor, K. Breitsprecher, J. de Graaf, M. Kuron, J. Landsgesell, H. Menke, D. Sean, and C. Holm, Espresso 4.0—an extensible software package for simulating soft matter systems, *The European Physical Journal Special Topics* **227**, 1789 (2019).
 - [49] W. T. Coffey, Y. P. Kalmykov, and J. T. Waldron, *The Langevin equation: with applications to stochastic problems in physics, chemistry and electrical engineering* (World Scientific, Singapore, 2004).
 - [50] J. D. Weeks, D. Chandler, and H. C. Andersen, Role of repulsive forces in determining the equilibrium structure of simple liquids, *J. Chem. Phys.* **54**, 5237 (1971).
 - [51] J. L. García-Palacios and F. J. Lázaro, Langevin-dynamics study of the dynamical properties of small magnetic particles, *Physical Review B* **58**, 14937 (1998).
 - [52] J. J. Cerda, V. Ballenegger, O. Lenz, and C. Holm, P3m algorithm for dipolar interactions, *The Journal of chemical physics* **129**, 234104 (2008).